Available online at www.sciencedirect.com
SCIENCE DIRECT
Journal of Power Sources 157 (2006) 494–500
JOURNAL OF POWER SOURCES
www.elsevier.com/locate/jpowsour

Structural and electrochemical properties of $LiNi_{1/3}Mn_{1/3}Co_{1/3}O_{2-x}F_x$ prepared by solid state reaction

Masaya Kageyama [a], Decheng Li [b], Koichi Kobayakawa [a], Yuichi Sato [a,*], Yun-Sung Lee [c]

[a] *Department of Applied Chemistry, Faculty of Engineering, Kanagawa University, 3-27-1 Rokkakubashi, Kanagawa-ku, Yokohama 221-8686, Japan*
[b] *High-Tech Research Center, Kanagawa University, 1-1-40 Suehiromachi, Tsurumi-ku, Yokohama 230-0045, Japan*
[c] *Faculty of Applied Chemistry, Chonnam National University, 300 Yongbong Dong, Kwangju 500-757, South Korea*

Received 24 May 2005; received in revised form 4 August 2005; accepted 10 August 2005
Available online 12 September 2005

Abstract

A series of $LiNi_{1/3}Mn_{1/3}Co_{1/3}O_{2-x}F_x$ ($0 \le x \le 1$) compounds was prepared by a solid state reaction and their characteristics were investigated by XRD, SEM, XPS, EIS, and charge–discharge test. The substitution of oxygen by fluorine produces change in the valences of the transition metal ions, thereby induces a complex change in the lattice parameters. Moreover, the fluorine doping of the $LiNi_{1/3}Mn_{1/3}Co_{1/3}O_2$ can promote the grain size growth and improve its crystallinity. The substituted samples with a low fluorine content can stabilize the interface between the surface layer of the active particles and the electrolyte after cycling, which is probably related to the improvement of the cyclic performance. A high fluorine content introduction into $LiNi_{1/3}Mn_{1/3}Co_{1/3}O_2$ significantly decreases its electrochemical properties, which is probably due to the formation of a new unstable interface as well as a structural instability caused by the nonequivilent substitution.

Keywords: Lithium-ion battery; Cathode material; $LiNi_{1/3}Mn_{1/3}Co_{1/3}O_{2-x}F_x$; Solid state reaction; Structural and electrochemical properties

1. Introduction

A layered compound, $LiNi_{1/3}Mn_{1/3}Co_{1/3}O_2$, is of great interest as a promising cathode material for lithium secondary batteries and has been intensively investigated, since it was first proposed by Ohzuku et al. [1–10]. It shows a reversible capacity of about 200 mAh g^{-1} in the range of 2.5–4.6 V as well as an excellent rate capability and good thermal stability [2]. The redox couples of $Li_xNi_{1/3}Mn_{1/3}Co_{1/3}O_2$ during charge–discharge cycling have been ascribed to Ni^{2+}/Ni^{3+} and Ni^{3+}/Ni^{4+} in the range of $2/3 \le x \le 1$ and $1/3 \le x \le 2/3$, respectively. The valence of Mn remains tetravalent during the entire process [3]. However, the Co^{3+}/Co^{4+} couple during the charge and discharge process is still a controversial issue. Ceder and co-workers [3] and Chowdari and co-workers [4] suggested that the redox reaction is in the range of $0 \le x \le 1/3$, whereas Kim and Chung [5] believed that the Co^{3+}/Co^{4+} reaction seemed to occur over the entire range of x in the $Li_xNi_{1/3}Mn_{1/3}Co_{1/3}O_2$. Moreover, McBreen and co-workers [6] reported that a large portion of the charge compensation during charging was achieved at the oxygen site although the cobalt was involved in the redox process.

The unsatisfactory cyclic performance in the range of 2.5–4.6 V is one of the problems of $LiNi_{1/3}Mn_{1/3}Co_{1/3}O_2$, whose mechanism has not yet been clarified. Recently, Sun et al. [11,12] reported that the fluorine-substituted $LiNi_{1/3}Mn_{1/3}Co_{1/3}O_2$ would exhibit an improved cyclability in this range. A study of the structural and electrochemical characteristics of this system is helpful in order to elucidate the capacity fading mechanism.

* Corresponding author. Tel.: +81 45 481 5661x3885; fax: +81 45 413 9770.
E-mail address: satouy01@kanagawa-u.ac.jp (Y. Sato).

0378-7753/$ – see front matter © 2005 Elsevier B.V. All rights reserved.
doi:10.1016/j.jpowsour.2005.08.002

In the present study, a series of $LiNi_{1/3}Mn_{1/3}Co_{1/3}O_{2-x}F_x$ ($0 \leq x \leq 1$) compounds was prepared by a solid state reaction. We also characterized their structural and electrochemical properties.

2. Experimental

$LiOH{\cdot}H_2O$ (Kishida), LiF (Kishida), γ-MnOOH (Tosoh), $Ni(OH)_2$ (Wako), and CoO (Wako) were selected as the starting materials. After being automatically ground and thoroughly mixed, these stoichiometric compounds were pressed into pellets and sintered at 950 °C for 15 h in air and then cooled to room temperature in a furnace.

The XRD measurements were carried out using a Rigaku Rint1000 diffractometer equipped with a monochromator and Cu target tube.

The scanning electron microscope (SEM) study of the samples was performed using a Hitachi S-4000 electron microscope.

The surface properties of sample particles were investigated by X-ray photoelectronic spectroscopy (XPS) using a JPS-9010 instrument.

The charge/discharge tests were carried out using the CR2032 coin-type cell, which consisted of a cathode and lithium metal anode separated by a Celgard 2400 porous polypropylene film. The cathode contains a mixture of 20 mg of accurately weighed active materials and 13 mg of the teflonized acetylene black (TAB-2) as the conducting binder. The mixture was pressed onto stainless mesh and dried at 130 °C for 5 h. The cells were assembled in a glove box filled with dried argon gas. The electrolyte was 1 M $LiPF_6$ in ethylene carbonate/dimethyl carbonate (EC/DMC, 1:2, v/v).

The electrochemical impedance spectroscopy (EIS) were carried out using a home-made tri-electrode cell using metallic lithium as the counter and reference electrodes with 1 M $LiPF_6$ in ethylene carbonate/dimethyl carbonate (EC/DMC, 1:2, v/v) as the electrolyte. Three milligrams of the active material was well mixed with 2 mg TAB-2 and pressed onto a stainless mesh with an area of about 0.75 cm^2.

3. Results and discussion

Fig. 1 shows SEM images of $LiNi_{1/3}Mn_{1/3}Co_{1/3}O_{2-x}F_x$ prepared at 950 °C. It should be pointed out that all of the fluorine contents mentioned in this study refer to the nominal content. $LiNi_{1/3}Mn_{1/3}Co_{1/3}O_2$ exhibits an agglomerated morphology and the size of the primary particles is about 200 μm. As the fluorine content increases, the particles become well-shaped and their size significantly increases. The average size is about 2 μm for the sample with $x > 0.08$. These results suggest that fluorine substitution can improve the crystallinity of $LiNi_{1/3}Mn_{1/3}Co_{1/3}O_{2-x}F_x$. Recently, Jouanneau and Dahn [13] suggested that the LiF addition into $Li[Ni_xCo_{1-2x}Mn_x]O_2$ with $x = 0.1$ and 0.25 could increase the pellet density and electrode density. Our results confirm

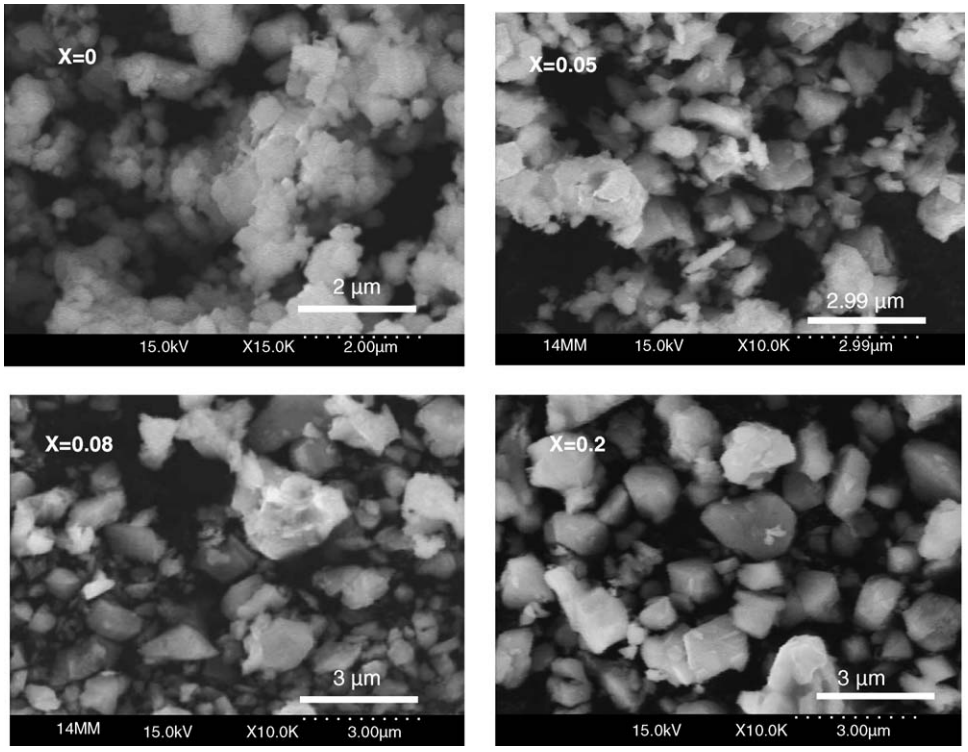

Fig. 1. SEM images of $LiNi_{1/3}Mn_{1/3}Co_{1/3}O_{2-x}F_x$ prepared at 950 °C.

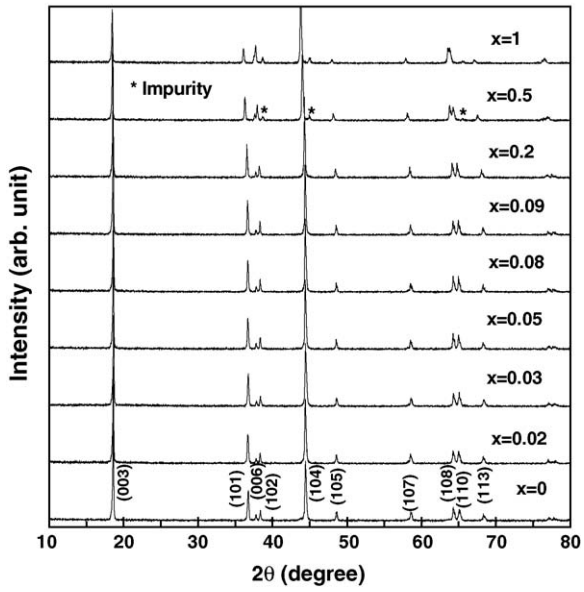

Fig. 2. XRD patterns of $LiNi_{1/3}Mn_{1/3}Co_{1/3}O_{2-x}F_x$ prepared at 950 °C.

this effect since $LiNi_{1/3}Mn_{1/3}Co_{1/3}O_2$ could be considered as a compound in $Li[Ni_xCo_{1-2x}Mn_x]O_2$ with $x = 1/3$.

Fig. 2 shows the XRD profiles of $LiNi_{1/3}Mn_{1/3}Co_{1/3}O_{2-x}F_x$ ($0 \le x \le 1$). Samples with $x < 0.5$ show the pure and typically layered features in terms of their XRD patterns, and all peaks can be indexed on the basis of the α-$NaFeO_2$ structure. New diffraction peaks were observed at 38°, 45°, and 66° in the samples with $x \ge 0.5$, which were not reported in Sun's work [11] although they addressed the fact that impurity phase appeared in the sample of $x > 0.15$. Since Noguchi and co-workers [14] reported that the electrochemical properties of $LiNi_{1/3}Mn_{1/3}Co_{1/3}O_2$ depended on the preparation method, we herein believed that the difference between our work and Sun's work probably results from the difference in the preparation method. Since its diffraction pattern is similar to that of α-$LiFeO_2$ [15], we deduce that this new phase probably has a disordered rock-salt structure. The origin of these new peaks is not very clear. We presume that its appearance should be related to the charge compensation during the substitution of fluorine for oxygen in $LiNi_{1/3}Mn_{1/3}Co_{1/3}O_2$. It is well known that charge compensation will occur when O^{2-} is replaced by F^- in order to keep the compound in electronic neutrality, which would probably cause the decrease in the average valence of the transition metals in $LiNi_{1/3}Mn_{1/3}Co_{1/3}O_2$. If the fluorine content is over some specific value (for example, $x = 0.5$ in $LiNi_{1/3}Mn_{1/3}Co_{1/3}O_{2-x}F_x$), the charge compensation through the decrease in the average valence of the transition metals could not meet the requirement of neutrality. Therefore, a new phase will form.

Moreover, a closer inspection of the change in the (0 0 3) and (1 1 0) peaks, which is shown in Fig. 3, reveals that the (1 1 0) peak monotonously shifts to a low angle as the fluorine content increases while the (0 0 3) peak initially shifts to a

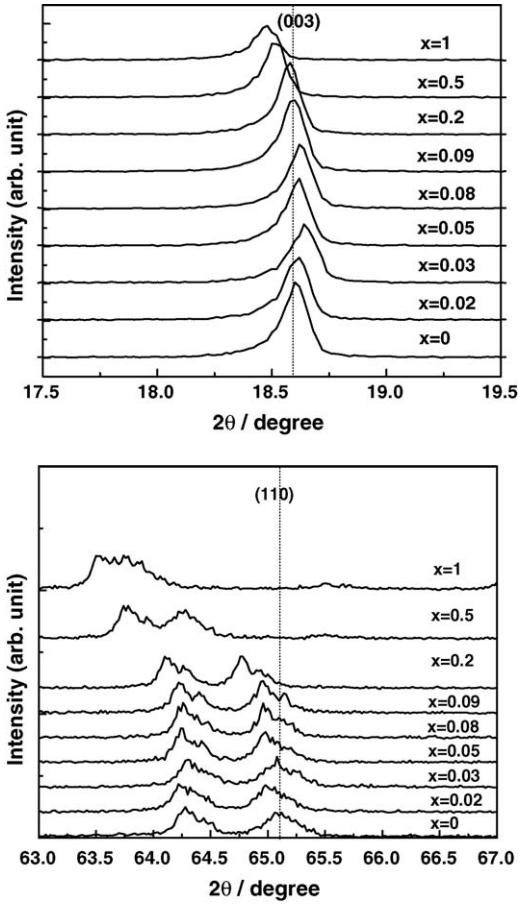

Fig. 3. Enlarged diffraction profiles of (0 0 3) and (1 1 0) peaks of $LiNi_{1/3}Mn_{1/3}Co_{1/3}O_{2-x}F_x$.

high angle when $x < 0.05$ and then goes back to low angle when $x > 0.08$. These results imply that the substitution of fluorine for oxygen causes an expansion in an axis whereas it initially induces shrinkage in the c axis and then expansion when $x > 0.08$.

The lattice parameters of $LiNi_{1/3}Mn_{1/3}Co_{1/3}O_{2-x}F_x$ ($0 \le x \le 1$) were roughly calculated by a least squares method using 10 diffraction lines, and these results are shown in Fig. 4. The lattice parameters, a and c, are 2.862 Å and 14.37 Å, respectively for $LiNi_{1/3}Mn_{1/3}Co_{1/3}O_2$, and in good agreement with reported results [2,14]. As fluorine content increases, lattice parameter, a, remains at a constant value of 2.868 Å from $x = 0.02$ to 0.2, slightly higher than that of the $LiNi_{1/3}Mn_{1/3}Co_{1/3}O_2$. As the fluorine content further increases, it significantly increases to 2.896 Å and 2.920 Å for $x = 0.5$ and 1.0, respectively. In the case of lattice parameter c, it initially decreases from 14.37 Å for $x = 0$ to 14.27 Å for $x = 0.03$ and then continuously increases as x increases. The values of c are 14.37 Å and 14.38 Å for $x = 0.5$ and 1.0, respectively, nearly the same as the undoped sample. The change in the cell volume follows the change in the c axis. The variation in lattice parameters with the fluorine content seems to be puzzling. It is well known that the small size of a dopant induces a decrease in the lattice parameter for a solid

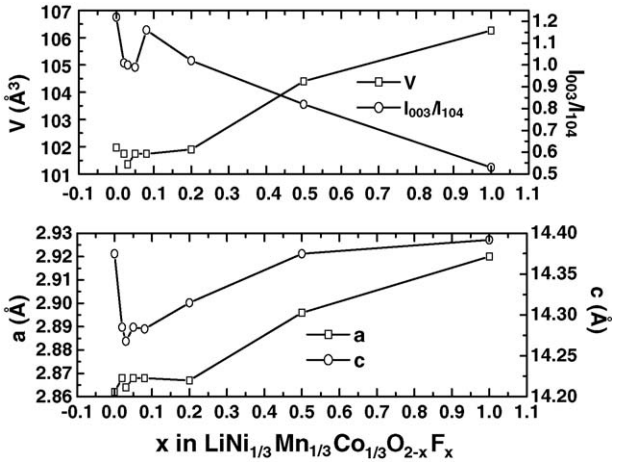

Fig. 4. Lattice parameters of $LiNi_{1/3}Mn_{1/3}Co_{1/3}O_{2-x}F_x$ vs. fluorine content, x.

solution system according to Vegard's Law; thus, the substitution of fluorine for oxygen should reduce lattices parameters, given that the radius of F^- (1.34 Å) is smaller than that of O^{2-} (1.40 Å) [11]. However, it should be pointed that the charge compensation from transition metal ions should occur in order to remain the electronic neutrality when O^{2-} ions are replaced by F^-. This probably gives rise to an increase in the content of the transition metal ions with a low valence and results in the expansion in the lattice volume, as observed in $LiAl_xMn_{2-x}O_{4-z}F_z$ [16]. We believe that Vegard's Law is hold in the case of a low content substitution while the influence of charge compensation from the transition metal ions becomes pronounced as the fluorine content increases.

Fig. 5 shows the XPS spectra of Ni ($2p^{3/2}$), Mn ($2p^{3/2}$), and Co($2p^{3/2}$) of $LiNi_{1/3}Mn_{1/3}Co_{1/3}O_{2-x}F_x$ ($x = 0, 0.03, 0.08$, 0.15, and 0.2). These profiles were recorded after the samples were ion-etched for 30 s. The published binding energies of the Ni^{2+}, Ni^{3+}, Mn^{3+}, Mn^{4+}, and Co^{3+} were provided as a reference [4]. The oxidation states of Ni and Co in $LiNi_{1/3}Mn_{1/3}Co_{1/3}O_2$ are mainly 2+ and 3+, the same as those reported results [4]. The valence of Mn is 3+, lower than it should be (tetravalent). This implies that our sample deviates from the ideal $LiNi_{1/3}Mn_{1/3}Co_{1/3}O_2$. In the case of $LiNi_{1/3}Mn_{1/3}Co_{1/3}O_{1.97}F_{0.03}$, the spectra of Ni ($2p^{3/2}$), Mn ($2p^{3/2}$), and Co ($2p^{3/2}$) shift to a high binding energy, indicating that the valences of Ni, Mn, and Co increase, well consistent with the reducing in the lattice parameter c, and V decreases for samples with $x < 0.05$. The contents of Ni^{2+}, Mn^{3+}, and Co^{3+} slightly increase as the fluorine content increases. These results confirm our assumption in the structure analysis for the samples with a high fluorine content.

As far as the slight increase in lattice parameter a is concerned, we found that the intensity ratio of (0 0 3) to (1 0 4) illustrated in Fig. 3, which is sensitive to the cation mixing in such a layered structure [17], decreases as x increases. This probably means that some Li^+ ions occupy the sites where transition metal ions should be. We believe that the large size

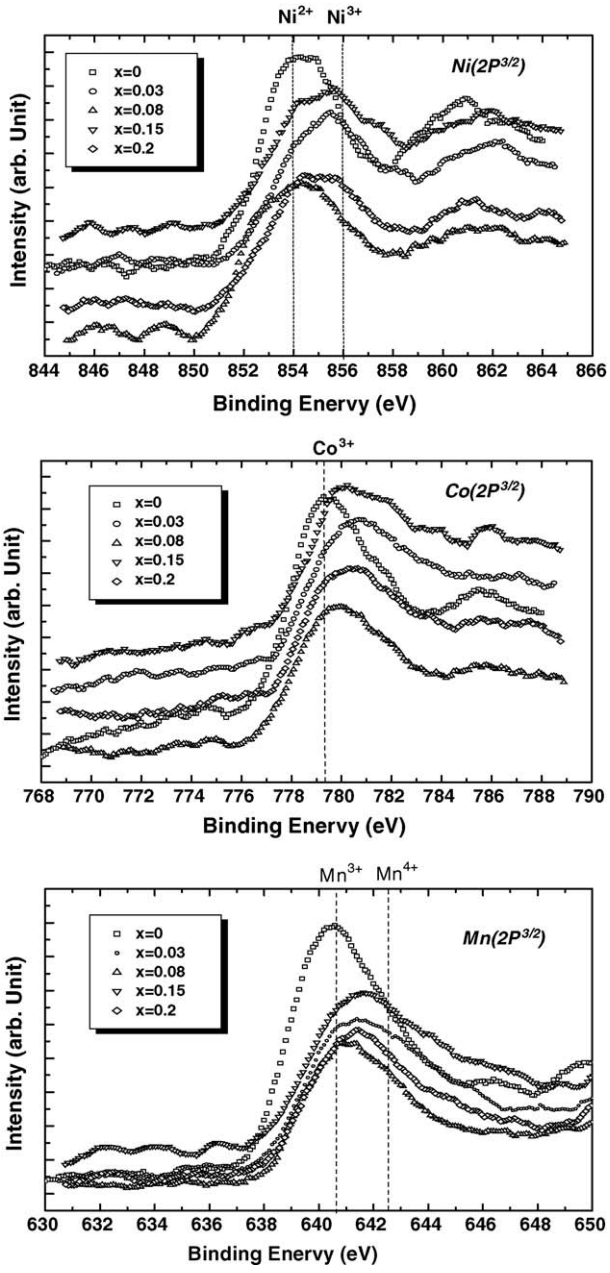

Fig. 5. XPS spectra of Ni, Mn and Co in $LiNi_{1/3}Mn_{1/3}Co_{1/3}O_{2-x}F_x$.

of Li^+ together with the increase in the low valent metal ions are attributed to the increase in the lattice parameter, a.

Fig. 6 shows the XPS spectra of F(1 s) of $LiNi_{1/3}Mn_{1/3}Co_{1/3}O_{2-x}F_x$ ($x = 0.08$, 0.15, and 0.2) recorded after different etching times. In the case of the $LiNi_{1/3}Mn_{1/3}Co_{1/3}O_{1.92}F_{0.08}$, the intensity of F (1 s) is rather low before etching and becomes undetectable after being etched for 30 s and 60 s. This suggests that the fluorine is mainly distributed on the surface of the particles. In $LiNi_{1/3}Mn_{1/3}Co_{1/3}O_{1.85}F_{0.15}$ and $LiNi_{1/3}Mn_{1/3}Co_{1/3}O_{1.8}F_{0.2}$, the intensities of F (1 s) become enhanced after being ion-etched, and seem to be independent of the etching time. These results suggest that the fluorine is successfully doped

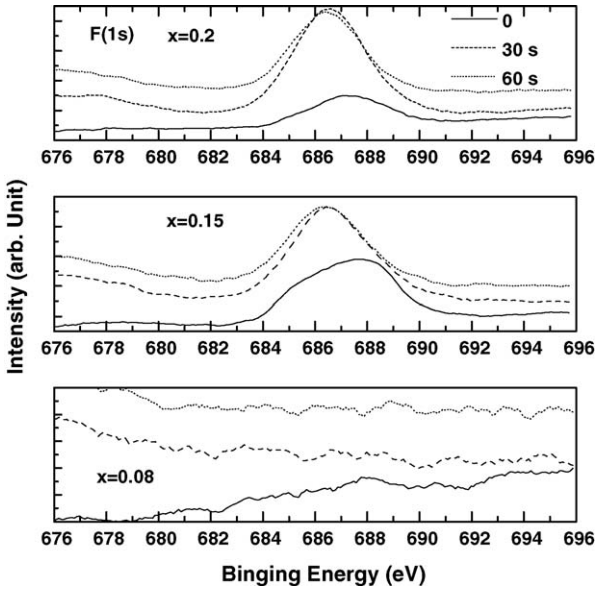

Fig. 6. XPS spectra of F(1 s) in $LiNi_{1/3}Mn_{1/3}Co_{1/3}O_{2-x}F_x$.

into the lattice of $LiNi_{1/3}Mn_{1/3}Co_{1/3}O_{1.85}F_{0.15}$ and $LiNi_{1/3}Mn_{1/3}Co_{1/3}O_{1.8}F_{0.2}$. Moreover, the content and the electronic state of fluorine on the surface of these particles seems to be different from those in the bulk in terms of the integrate area and the binding energy. We believe that the fluorine distribution in the ideal $LiNi_{1/3}Mn_{1/3}Co_{1/3}O_{2-x}F_x$ should be homogeneous from the surface to the core of the particles, although our experimental results suggested an inhomogeneous distribution. We think this abnormal phenomenon is originating from the experimental errors induced during samples preparation, such as bad mixing of the starting materials; an inhomogeneous temperature distribution in the oven because it has been pointed out that the preparation of the Li–Ni–Mn–Co–O system was significantly affected by the experimental conditions [13,14,18].

Fig. 7 shows the cyclic performance of $LiNi_{1/3}Mn_{1/3}Co_{1/3}O_{2-x}F_x$ operating at a current density of 0.4 mA cm^{-2} in 2.5–4.5 V. $LiNi_{1/3}Mn_{1/3}Co_{1/3}O_2$ shows a reversible capacity of about 140 mAh g^{-1}, about 87% of its initial discharge capacity (160 mAh g^{-1}). The influence of the fluorine substitution on the cyclic performance of $LiNi_{1/3}Mn_{1/3}Co_{1/3}O_{2-x}F_x$ is complex. Generally, the reversible capacities

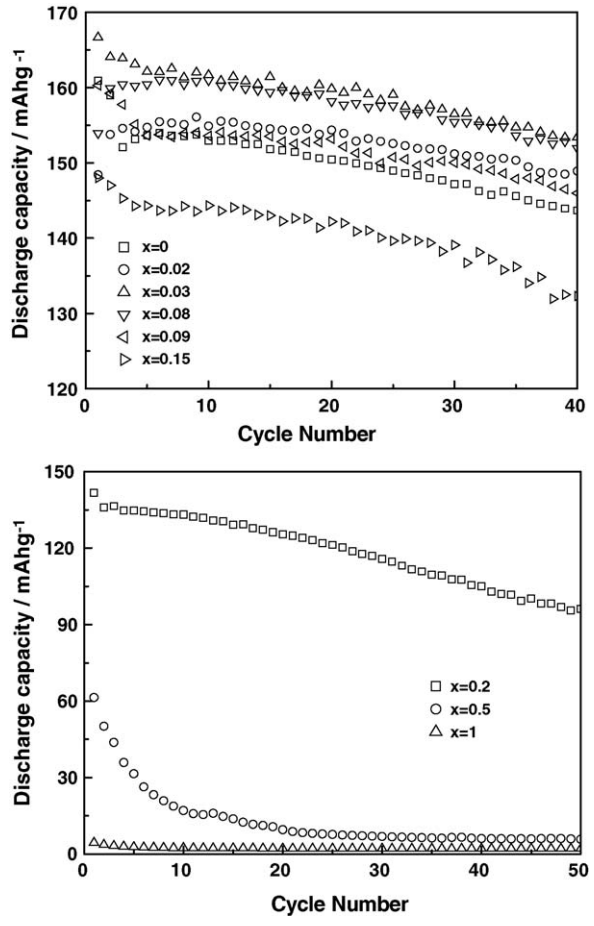

Fig. 7. Reversible capacities of $LiNi_{1/3}Mn_{1/3}Co_{1/3}O_{2-x}F_x$ vs. cycle number at a current density of 0.4 mA cm^{-2} in 2.5–4.5 V range.

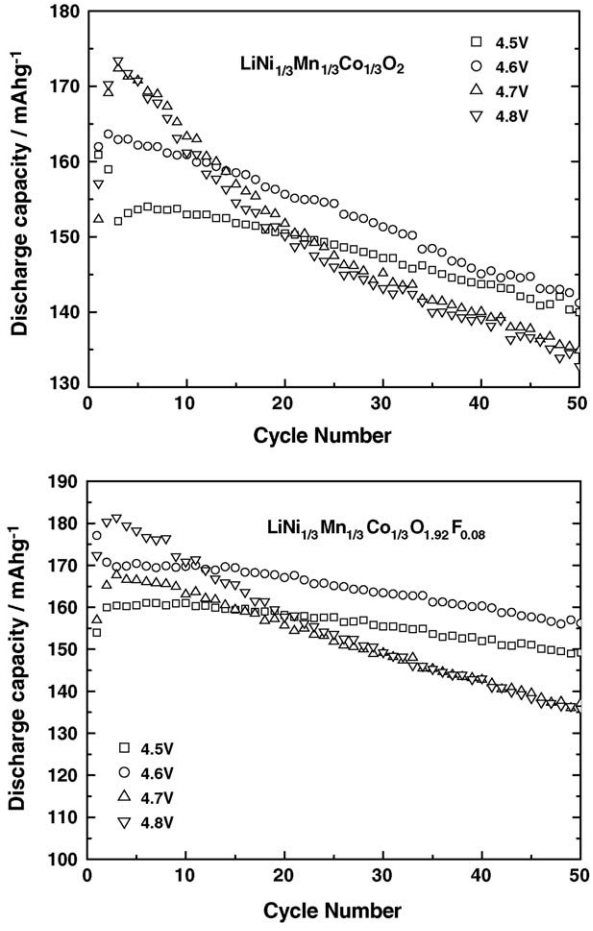

Fig. 8. Cyclic performances of $LiNi_{1/3}Mn_{1/3}Co_{1/3}O_2$ and $LiNi_{1/3}Mn_{1/3}Co_{1/3}O_{1.92}F_{0.08}$ operating at different cutoff voltages.

of $LiNi_{1/3}Mn_{1/3}Co_{1/3}O_{2-x}F_x$ increase at x less than 0.15 and more than 90% initial discharge capacities can be retained, indicating that the fluorine introduction indeed improved the cyclic performance. For samples with $x \geq 0.15$, both the initial discharge capacity and reversible capacity decrease, suggesting that the doping of fluorine at a high level significantly deteriorates the electrochemical performance of $LiNi_{1/3}Mn_{1/3}Co_{1/3}O_{2-x}F_x$. Moreover, for $LiNi_{1/3}Mn_{1/3}Co_{1/3}O_{1.98}F_{0.02}$ and $LiNi_{1/3}Mn_{1/3}Co_{1/3}O_{1.92}F_{0.08}$, the discharge capacities initially increase and then gradually decrease after 10 cycles, whereas other samples undergo a quick capacity loss in the first several cycles before reaching a stable electrochemical performance. Thackeray and co-workers [19] had observed the existence of "conditioning cycles" in the $LiNi_{0.5}Mn_{0.5}O_2$ and $0.95LiNi_{0.5}Mn_{0.5}O_2{\cdot}0.05Li_2TiO_3$ electrodes and ascribed it to the instability of the delithiated electrode surface induced by oxygen loss.

Fig. 8 shows the cyclic performances of $LiNi_{1/3}Mn_{1/3}Co_{1/3}O_2$ and $LiNi_{1/3}Mn_{1/3}Co_{1/3}O_{1.92}F_{0.08}$ operating at the different cutoff voltages for a current density of 0.2 mA cm^{-2}. $LiNi_{1/3}Mn_{1/3}Co_{1/3}O_2$ shows a significant capacity fading when the cutoff voltage is 2.5–4.6 V. The higher the cutoff voltage, the poorer the cyclic performance. $LiNi_{1/3}Mn_{1/3}Co_{1/3}O_{1.92}F_{0.08}$ exhibits an improved cyclability compared to $LiNi_{1/3}Mn_{1/3}Co_{1/3}O_2$ when it is cycling at 2.4–4.6 V. However, its capacity fading becomes severe when the cutoff voltage is over 4.7 V. Since the capacity fading mechanism in the high cutoff voltage range is still unclear, further efforts are necessary to elucidate this issue.

Fig. 9 shows the cyclic performance of $LiNi_{1/3}Mn_{1/3}Co_{1/3}O_2$ and $LiNi_{1/3}Mn_{1/3}Co_{1/3}O_{1.92}F_{0.08}$ operating at different current densities. The cyclability of $LiNi_{1/3}Mn_{1/3}Co_{1/3}O_2$ seems to be independent of the current density since its retentive capacities are nearly the same after 50 cycles when the current density increases from 0.1 mA cm^{-2} to 1.2 mA cm^{-2}. In the case of the $LiNi_{1/3}Mn_{1/3}Co_{1/3}O_{1.92}F_{0.08}$, its reversible capacity is 162 mAh g^{-1} and almost no capacity fading was observed (the initial discharge capacity is about 166 mAh g^{-1}). However, its cyclic performance degrades as the current density increases.

Fig. 10 shows the Cole-Cole plots of pristine $LiNi_{1/3}Mn_{1/3}Co_{1/3}O_{2-x}F_x$ ($x = 0$, 0.08, and 0.2) electrodes and after two cycles. A semicircle was observed

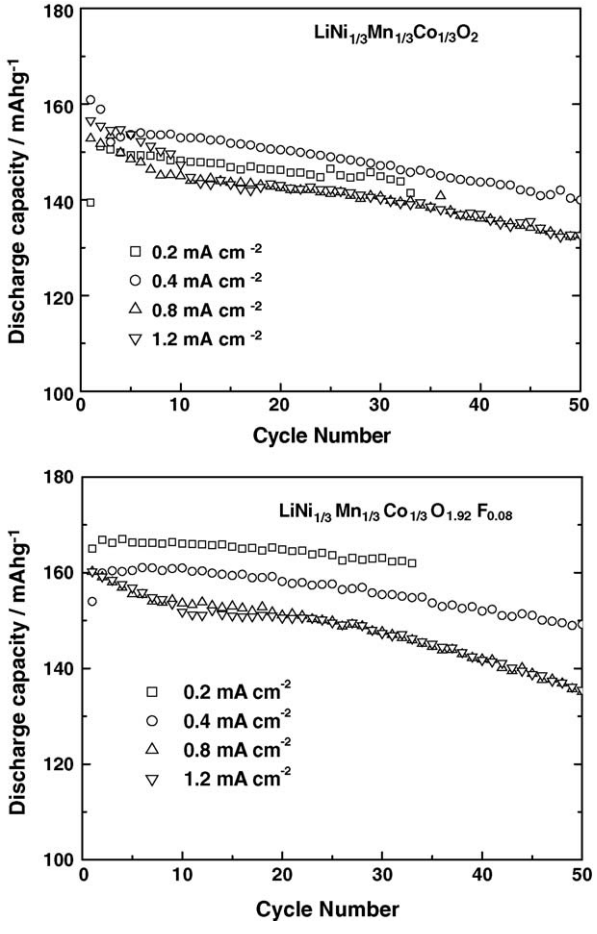

Fig. 9. Cyclic performances of $LiNi_{1/3}Mn_{1/3}Co_{1/3}O_2$ and $LiNi_{1/3}Mn_{1/3}Co_{1/3}O_{1.92}F_{0.08}$ operating at different current densities in the 2.5–4.5 V range.

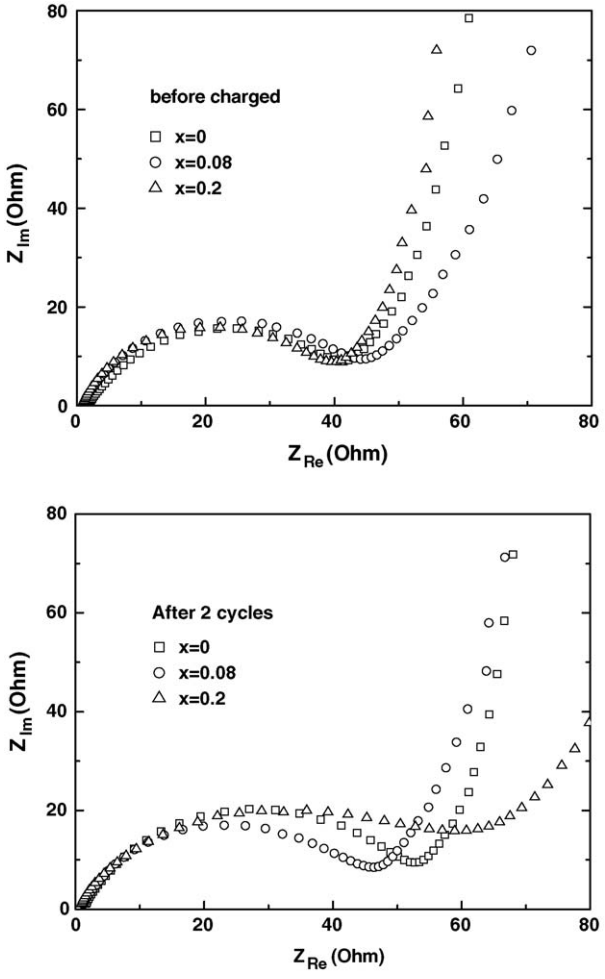

Fig. 10. Cole–Cole plots of pristine $LiNi_{1/3}Mn_{1/3}Co_{1/3}O_{2-x}F_x$ ($x = 0$, 0.08 and 0.2) electrodes before charged and after two cycles.

in high frequency domain for all samples in the pristine state and its origin is probably related to the lithium ion migration through the interface between the surface layer of the particles and the electrolyte [20,21]. After two cycles, the $LiNi_{1/3}Mn_{1/3}Co_{1/3}O_{1.92}F_{0.08}$ shows the most stable surface layer due to the unchanged resistance while this resistance slightly increases for $LiNi_{1/3}Mn_{1/3}Co_{1/3}O_2$. The semicircle of $LiNi_{1/3}Mn_{1/3}Co_{1/3}O_{1.8}F_{0.2}$ becomes depressed and elongated, which implying that a new interface appears probably after cycling. The EIS analysis results, combined with the cyclic performances of $LiNi_{1/3}Mn_{1/3}Co_{1/3}O_{2-x}F_x$ were done at different current densities and for different cutoff voltages, suggest that the mechanism of the capacity fading of at the high cutoff voltages of $LiNi_{1/3}Mn_{1/3}Co_{1/3}O_2$ is probably due to the instability of the delithiated electrode surface. The substitution of fluorine for oxygen can stabilize the interface between the electrolyte and the surface layer of the particles when the fluorine content is low. However, this interface becomes unstable when the electrodes were operated at a high current density. The high fluorine content in $LiNi_{1/3}Mn_{1/3}Co_{1/3}O_{2-x}F_x$ significantly decreases the cyclic performances of $LiNi_{1/3}Mn_{1/3}Co_{1/3}O_{2-x}F_x$, which is probably related to the formation of a new unstable interface as well as a structural instability resulting from the nonequivalent substitution.

4. Conclusion

$LiNi_{1/3}Mn_{1/3}Co_{1/3}O_{2-x}F_x$ ($0 \le x \le 1$) was prepared by a solid state reaction and the impacts of the fluorine substitution for oxygen in $LiNi_{1/3}Mn_{1/3}Co_{1/3}O_2$ on its crystal structure, morphology and surface properties, and electrochemical characteristics have been systematically investigated. Although the preparation of $LiNi_{1/3}Mn_{1/3}Co_{1/3}O_{2-x}F_x$ by a solid state reaction is prone to be affected by the experimental conditions, the fluorine doping into $LiNi_{1/3}Mn_{1/3}Co_{1/3}O_2$ did induce complex variations in its lattice parameters and surface properties. The substitution of fluorine for oxygen in $LiNi_{1/3}Mn_{1/3}Co_{1/3}O_2$ also promotes the particle growth and improves the crystallinity of $LiNi_{1/3}Mn_{1/3}Co_{1/3}O_{2-x}F_x$.

The cyclic performances of $LiNi_{1/3}Mn_{1/3}Co_{1/3}O_2$ and $LiNi_{1/3}Mn_{1/3}Co_{1/3}O_{2-x}F_x$ depend on the operating current densities and the cutoff voltages. Since Yabuuchi and Ohzuku [2] and Noguchi and co-workers [14] reported that the volume change of $LiNi_{1/3}Mn_{1/3}Co_{1/3}O_2$ was very small during cycling at 3–4.6 V, the possibility resulting from the instability of its bulk structure is low. Thus, we believe that the deterioration of the cyclability at a high current density and/or in a high cutoff voltage range should be attributed to the instability of the surface layer between the active particles and the electrolyte solution. This seems to imply that the key to improving the cyclability of $LiNi_{1/3}Mn_{1/3}Co_{1/3}O_2$ is to enhance the stability of this surface layer by either ionic substitution or surface modification.

Acknowledgement

This work was financially supported by the High-Tech Research Center Project for Private University: matching fund subsidy from the Ministry of Education, Culture, Sports, Science and Technology (MEXT) from 2001 to 2005.

References

[1] T. Ohzuku, Y. Makimura, Chem. Lett. 642 (2001).
[2] N. Yabuuchi, T. Ohzuku, J. Power Sources 119 (2003) 171.
[3] B.J. Hwang, Y.W. Tsai, D. Carlier, G. Ceder, Chem. Mater. 15 (2003) 3676.
[4] K.M. Shaju, G.V. Subba Rao, B.V.R. Chowdari, Electrochim. Acta 48 (2002) 145.
[5] J. Kim, H. Chung, Electrochim. Acta. 49 (2004) 937.
[6] W. Yoon, C.P. Grey, M. Balasubramanian, X. Yang, D.A. Fischer, J. McBreen, Electrochem. Solid-State Lett. 7 (2004) 53.
[7] Y.M. Todorov, K. Numata, Electrochim. Acta 50 (2004) 493.
[8] S.H. Park, C.S. Yoon, S.G. Kang, H.-S. Kim, S.-I. Moon, Y.-K. Sun, Electrochim. Acta 49 (2004) 557.
[9] T. Cho, S. Park, M. Yoshio, Chem. Lett. 33 (2004) 704.
[10] J. Choi, A. Manthiram, Electrochem. Solid-State Lett. 7 (2004) 365.
[11] S. Myung, G. Kim, Y. Sun, Chem. Lett. 33 (2004) 1388.
[12] G. Kim, S. Myung, H. Bang, Jai. Prakash, Y. Sun, Electrochem. Solid-State Lett. 7 (2004) 447.
[13] S. Jouanneau, J.R. Dahn, J. Electrochem. Soc. 151 (2004) 1749.
[14] D. Li, T. Muta, L. Zhang, M. Yoshio, H. Noguchi, J. Power Sources 132 (2004) 150.
[15] Y. Sakurai, H. Arai, J. Yamaki, Solid State Ionics 113–115 (1998) 29.
[16] G.G. Amatucci, N. Pereira, T. Zheng, J.-M. Tarascon, J. Electrochem. Soc. 148 (2001) 171.
[17] T. Ohzuku, A. Ueda, M. Nagayama, J. Electrochem. Soc. 140 (1993) 1862.
[18] M. Yoshio, Y. Todorov, K. Yamato, H. Noguchi, J. Itoh, M. Okada, T. Mouri, J. Power Sources 74 (1998) 46.
[19] J.-S. Kim, C.S. Johnson, M.M. Thackeray, Electrochem. Commun. 4 (2002) 205.
[20] D. Aurbach, M. Levi, E. Levi, H. Teller, B. Markovsky, G. Salitra, U. Heider, L. Heider, J. Electrochem. Soc. 145 (1998) 3024.
[21] M. Levi, G. Salitra, B. Markovsky, H. Teller, D. Aurbach, U. Heider, L. Heider, J. Electrochem. Soc. 146 (1999) 1279.